Available online at www.sciencedirect.com
SCIENCE DIRECT
Catalysis Today 105 (2005) 701–708
CATALYSIS TODAY
www.elsevier.com/locate/cattod

Combustion of methane lean mixtures in reverse flow reactors: Comparison between packed and structured catalyst beds

Pablo Marín, Miguel A.G. Hevia, Salvador Ordóñez *, Fernando V. Díez

Department of Chemical and Environmental Engineering, University of Oviedo, Julián Clavería s/n, 33071-Oviedo, Spain

Abstract

The scope of this work is to compare systematically the performance of particle beds and monolithic beds in catalytic reverse flow reactors used for combustion of lean methane/air mixtures, using alumina-supported palladium as catalyst. Different values of gas surface velocity (0.1–0.3 m/s), particle diameter (3–6 mm, for particle bed), cell density (200–400 cpsi, for structured bed) and catalyst/inert ratio (0.4–1) were used for the simulation of the combustion of 3500 ppm methane in both kinds of reverse flow reactor. An unsteady one-dimensional heterogeneous model has been developed and solved using a MATLAB code. The model, physical parameters and transport properties used had been experimentally validated in a previous work, operating with a particle bed reverse flow reactor. Results obtained indicate that the reverse flow reactor is more stable when the catalyst particle beds are use, although the difference with the monolith bed decreases as surface velocity increases. In contrast, pressure drops in the bed are higher for the particle bed.

Keywords: Catalytic combustion; Reactor modeling; Reverse-flow reactors; Particle bed reactors; Monolithic reactors

1. Introduction

Volatile organic compounds (VOCs) are an environmental problem because of both their intrinsic toxicity and their contribution to the formation of photochemical smog in urban areas. Although methane is formally excluded from the VOC definition because of its low activity as photochemical oxidants precursor, it appropriate as model compound for the study of the performance of combustion reactors, both catalytic and homogeneous, because it is more refractory to deep oxidation than most VOCs. Hence, a satisfactory operation with methane ensures a proper treatment for almost any VOC. Furthermore, methane is a very important greenhouse gas (the most important contributor to this effect after carbon dioxide), the main anthropogenic sources being livestock, landfills, natural gas and oil extraction and distribution systems, and coal mines. Global warming potential of methane over a 100 years period is estimated to be about 23 times higher than the corresponding to carbon dioxide, so there is a clear advantage from this point of view in transforming methane into carbon dioxide.

Catalytic combustion is among the most promising VOC treatment processes because it presents several advantages, particularly when compared with homogeneous combustion: the lower ignition temperatures required by the catalytic process lead to smaller equipments, lower pressure drops, less heat losses, and negligible rates of nitrogen oxides production [1]. In spite of this, energetic aspects play a key role in the development of catalytic oxidation reactors. Although involved reactions are exothermic, the low hydrocarbon concentrations lead this process to be often energy-consuming.

Reverse flow catalytic reactors (RFR) are a very interesting alternative proposed to overcome this problem. Catalytic RFR consist of a catalyst bed in which the feed flow direction is periodically reversed. So, using the adequate switching time, the combustion heat is kept inside the reactor. Usually, the catalyst is substituted at both ends of the bed, where the temperature is not high enough to achieve appreciable reaction rates, by an inert material with more

* Corresponding author. Tel.: +34 985 103 437; fax: +34 985 103 434.
E-mail address: sordonez@uniovi.es (S. Ordóñez).

0920-5861/$ – see front matter © 2005 Elsevier B.V. All rights reserved.
doi:10.1016/j.cattod.2005.06.003

List of symbols

a	surface–volume ratio (m^2/m^3)
A^{he}	pre-exponential factor for heterogeneous reaction ($m^3/s\ m^3$) cat
C	molar concentration (mol/m^3)
C_P	heat capacity (J/kg K)
d_P	particle bed particle diameter (mm)
$\langle d \rangle_{pores}$	catalyst pore mean diameter (m)
d_W	reactor wall thickness (m)
D_{AB}	methane–air molecular diffusion coefficient (m^2/s)
D_{eff}	axial mass dispersion coefficient (m^2/s)
D_H	hydraulic diameter (m)
D_K	Knudsen diffusion coefficient (m^2/s)
D_R	reactor internal diameter (m)
e	insulation thickness (m)
E_a^{he}	activation energy for heterogeneous reaction (J/mol)
$(E_{relative})_{max}$	maximum relative error comparing experimental and fitted data
f_{CB}	catalytic bed fraction in the entire reactor
f_C	catalyst fraction in the catalytic bed
h	gas–solid heat transfer coefficient ($W/m^2\ K$)
k	thermal conductivity (W/m K)
k_a	insulation thermal conductivity (W/m K)
K_G	gas–solid mass transfer coefficient (m/s)
k_S	kinetic constant per catalyst surface ($m^3/s\ m^2$)
k_{VC}	kinetic constant per catalyst volume ($m^3/s\ m^3$) cat
k_{eff}	axial effective thermal dispersion coefficient (W/m K)
L_C	effectiveness washcoat thickness (m)
L_R	reactor length (m)
M	molecular weight (kg/mol)
N_m	number of channels per area (cpsi)
P	pressure (Pa)
Q_G	gas flow (m^3/s)
$(r_A)_S^{he}$	heterogeneous reaction rate per catalyst surface ($mol/m^2\ s$)
$(r_A)_{VG}^{ho}$	homogeneous reaction rate per gas volume ($mol/m^3\ s$)
r^2	square regression coefficient
R	ideal gas constant (J/mol K)
T	temperature (°C)
t	temp independent variable (s)
t_{SW}	switching time (s)
u	surface velocity (m/s)
v	linear velocity (m/s)
y	methane molar fraction in the gas phase
z	axial length along the reactor (m)

Greek symbols

$\Delta\tilde{H}_R$	combustion enthalpy (J/mol)
ΔP	pressure drop (Pa)
ε	bed void fraction
ε_{pores}	pores void fraction
ϕ	Thiele modulus
η	internal effectiveness
μ	viscosity (kg/m s)
ρ	density (kg/m^3)
τ_{pores}	pore tortuosity

Sub indexes and super indexes

0	reactor inlet conditions
A	reaction compound (methane)
C	catalyst
G	gas phase
he	heterogeneous reaction
ho	homogeneous reaction
i	initial conditions
S	solid phase
W	reactor wall

adequate physical properties. The operation with this kind of reactors implies the preheating of the solid only during the start up stage. When the solid reaches a temperature higher than the ignition temperature of the compound to be burned, the gas mixture is fed to the reactor at room temperature. Combustion generates a temperature wave on the gas and on the solid, which creeps from the feed inlet to the outlet. In a certain moment, the feed flow is reversed, because otherwise the temperature wave would reach the limits of the bed, causing eventually the extinction of the reactor. Hence, at this point the gas mixture is fed from the opposite side of the reactor, where the heat stored is used to preheat the gas up to the ignition temperature. The main operation and control parameter of RFR is the switching or semicycle time (t_{SW}), which is the time elapsed between two consecutive flow reversals.

As a result, both extremes of the bed act as heat regenerators, and the level of energy efficiency reached in a RFR is closely related to the physical properties of the packing, in both the catalyst and inert sections [2]. This capability of keeping the hot front within the limits of the bed, allows the autothermal treatment of very lean VOC mixtures, without using auxiliary fuel. Extensive investigations on RFR, including both numerical simulations and experimental analysis, have been performed in the past thirty years and have been reviewed, for example, by Matros and Bunimovich [3].

The reactor bed can be either formed by particles or structured. The advantages of structured or monolithic supports in catalytic processes are well known: low pressure drop, greater mechanical strength, better mass transfer, minimal ‘channelling’ across the bed in uniform monoliths, and tolerance to gaseous emissions containing particles, as

long as they are small enough to pass trough the channels. Eigenberger and Nieken [4] confirmed that particle RFR maintain these advantages. On the other hand, structured beds may be more prone to extinction, due to worst gas–solid heat transfer.

The scope of this work is to carry out a systematic comparison between particle beds and structured beds for VOC combustion in reverse flow reactors. Studies are based on computer simulations using a model experimentally validated [9]. The influence of the most relevant operating conditions, such as bed configuration (particle size or cells density), surface velocity or bed fraction loaded with catalyst, were also considered. Maximum temperature reached in the reactor, critical or maximum switching time allowable for stable operation, and pressure drop in the reactor where determined for both configurations.

2. Mathematical model

2.1. Mathematical model formulation

The mathematical dynamic model developed for the combustion of methane in RFR is heterogeneous and one-dimensional. The model is heterogeneous in order to take into account the temperature difference between solid and fluid, which can be large in highly exothermic reactions and near the extremes of the bed. The only dimension taken into account in the model is the axial-one, because, for adiabatic reactors operating at the conditions of this work, temperature and velocity radial profiles are almost flat (except in the vicinity of the reactor wall), and hence the difference in the results between one-dimensional (much easier to solve) and two-dimensional models is very small.

The resulting mathematical dynamic model is constituted by a system of partial differential-algebraic equations. The differential equations are obtained from conservation equations, applied separately to the gas and solid phases, and the algebraic equations are the ones used to estimate the physical and transport properties.

The reactor is considered to be adiabatic, heat transfer from the reactor wall to the surroundings being neglected. On the other hand, it has been shown that in reverse flow reactors is important to take into account the influence of the wall itself. In this way, the heat is transferred from the catalytic bed to the wall, spreads axially along the wall, and is transferred to the inert part of bed, which is significantly cooler. This heat transfer from the hot catalyst to the cool inert bed through the reactor wall has a negative effect on the stability of the reactor, as has been demonstrated, for instance, by Hevia et al. [5]. Hence, the reactor stability increases as the reactor diameter increases and the wall thermal conductivity decreases. So, the behavior of laboratory scale reactors, with small diameter and a high thermal conductivity wall (i.e. constructed in steel), are strongly affected by this phenomenon, which must be taken into account in the simulation model. Ideal gas behavior for the gas phase is also assumed.

Mass balance for the gas phase:

$$\frac{\partial y_G}{\partial t} = -\frac{u_0}{\varepsilon}\frac{\rho_{G0}}{\rho_G}\frac{\partial y}{\partial z} + D_{eff}\frac{\partial^2 y_G}{\partial z^2} - a_G K_G (y_G - y_S) + \frac{(r_A)_{V_G}^{ho}}{C_G} \tag{1}$$

Energy balance for the gas phase:

$$\frac{\partial T_G}{\partial t} = -\frac{u_0}{\varepsilon}\frac{\rho_{G0}}{\rho_G}\frac{\partial T_G}{\partial z} + \frac{k_{Geff}}{\rho_G C_{PG}}\frac{\partial^2 T_G}{\partial z^2} - \frac{a_G h}{\rho_G C_{PG}}(T_G - T_S) - \frac{4h_{WG}}{\varepsilon D_R \rho_G C_{PG}}(T_G - T_W) + \frac{(r_A)_{V_G}^{ho}\Delta H_R}{\rho_G C_{PG}} \tag{2}$$

Energy balance for the solid phase:

$$\frac{\partial T_S}{\partial t} = \frac{k_{Seff}}{\rho_S C_{PS}}\frac{\partial^2 T_S}{\partial z^2} - \frac{a_S h}{\rho_S C_{PS}}(T_S - T_G) - \frac{4h_{WS}}{(1-\varepsilon)D_R \rho_S C_{PS}}(T_S - T_W) + \frac{a_S (r_A)_S^{he}\Delta H_R}{\rho_S C_{PS}} \tag{3}$$

Energy balance for the wall:

$$\frac{\partial T_W}{\partial t} = \frac{k_W}{\rho_W C_{PW}}\frac{\partial^2 T_W}{\partial z^2} + \frac{h_{WG}D_R(T_G - T_W) + h_{WS}D_R(T_S - T_W)}{\rho_W C_{PW} d_W (D_R + d_W)} \tag{4}$$

Mass balance for the solid phase (first order reaction kinetics):

$$y_S = \frac{y_G}{1 + (\eta k_S^{he}/K_G)} \qquad (r_A)_S^{he} = -\eta k_S^{he} C_G y_S,$$
$$C_G = \frac{P_G}{RT_G} \tag{5}$$

Boundary conditions (Danckwerts boundary conditions):

Inlet:

$$(y_G)_{0^-} = (y_G)_{0^+} - \frac{\varepsilon D_{eff}}{u_0}\left(\frac{\partial y_G}{\partial z}\right)_{0^+};$$
$$(T_G)_{0^-} = (T_G)_{0^+} - \frac{\varepsilon k_{Geff}}{u_0 \rho_{G0} C_{PG}}\left(\frac{\partial T_G}{\partial z}\right)_{0^+} \tag{6}$$
$$\left(\frac{\partial T_S}{\partial z}\right)_{z=0^+} = \left(\frac{\partial T_W}{\partial z}\right)_{z=0^+} = 0$$

Outlet:

$$\left(\frac{\partial y_G}{\partial z}\right)_{z=L_R} = \left(\frac{\partial T_G}{\partial z}\right)_{z=L_R} = \left(\frac{\partial T_S}{\partial z}\right)_{z=L_R} = \left(\frac{\partial T_W}{\partial z}\right)_{z=L_R} = 0 \tag{7}$$

The above-mentioned equations take into account the homogeneous reaction in the gas phase. In the case of methane combustion, homogeneous reaction is only significant at

very high temperatures (>800 °C). In this work, the reactor works at much lower temperature, so that homogeneous combustion can be neglected.

The proposed system of partial differential equations can be used to describe both particle and structured catalyst beds. The differences are taken into account in the physical properties and in the correlations used to estimate the transport properties.

2.2. Kinetic expressions

In the development of the model, pseudo-first order kinetics for the catalytic combustion of methane has been assumed. This assumption has been experimentally checked for the sphere-shaped Pd–Al_2O_3 catalyst, and the kinetic parameters determined. The catalyst was ground to a small particle size (100–250 μm) in order to avoid internal and external diffusional effects, and the light-off curve (methane conversion vs. temperature for a constant mass of catalyst) was obtained. It was observed that the data fitted well to a first order kinetics in our working interval (methane concentration lower than 5000 ppm, and temperature below 600 °C), the corresponding parameters being activation energy 1.125×10^5 J/mol and intrinsic pre-exponential factor 1.58×10^{11} m^3/s m^3 cat. Deactivation of the Pd–Al_2O_3 catalyst was observed for temperatures higher than 600 °C. So, the behavior of the catalyst is not adequately represented by these parameters at temperature higher than 600 °C.

In order to stress the influence of the structure of the bed in the performance of the RFR, the comparison between particle and structured catalyst beds in RFR is made considering similar catalyst and intrinsic kinetics in both cases. Due to the geometric differences between both support types, the reaction rates per pellet volume and per washcoat volume, for particle bed and structured support, respectively, have been considered in the model. The structured catalyst has been considered to be formed by a washcoat of Pd–Al_2O_3, for which (as a preliminary approach) the intrinsic activity per washcoat volume is taken as equal to the intrinsic activity per pellet volume of the particle catalyst. This assumption is supported in the literature (for structured and particle Pd–Al_2O_3 catalysts, the intrinsic kinetic constants are within 20% in most cases [6,7]). Concerning to the monolith geometry, channels with square shape with an effective washcoat thickness (L_C) of 46 μm, were considered, according to data frequently found in the bibliography [8]. A summary of the parameters and conditions considered can be found in Table 1.

Table 1
Operation parameters used in the simulation of the RFR

Feed methane concentration (y_{G0})	3500 ppmV (0.35%)
Feed temperature (T_{G0})	25 °C
Feed pressure (P_0)	1.2 bar
Reactor length (L_R)	0.5 m
Reactor diameter (D_R)	0.05 m
Reactor wall thickness (d_W)	0.0012 m
Reactor wall density (ρ_W)	7700 kg/m^3
Reactor wall heat capacity (C_{PW})	500 J/kg K
Reactor wall thermal conductivity (k_W)	19.51 W/m K
Preheating temperature (T_{Pre})	400 °C
Reaction heat for methane combustion (ΔH_R)	−802 500 J/mol
Pre-exponential factor (A^{he})	1.58×10^{11} m^3/s m^3 cat
Activation energy (E_a)	1.125×10^5 J/mol
Mean pore diameter ($\langle d \rangle_{pores}$)	6.377×10^{-9} m
Internal catalyst porosity (ε_{pores})	0.519
Catalyst tortuosity (τ_{pores})	2
Effective washcoat thickness (L_C)	46×10^{-6} m

Both for particle and structured beds, internal and external mass transfer resistances are taken into account, introducing the effectiveness factor (η) and the mass transfer coefficient (K_G), respectively, and using adequate expressions in each case. The Knudsen diffusion coefficient throughout the catalyst pores was introduced in the calculation of the Thiele modulus, leading to the expressions shown in Table 2.

2.3. Physical and transport properties

Methane concentration considered in this work is low enough for assuming that the gas phase properties are the corresponding to pure air, and ideal gas behaviour can also be assumed. Regarding the solid bed, physical properties change along the reactor because it is formed by three consecutive sections: upper inert, central catalytically active, and lower inert.

For particle bed operation, the active central part is considered to contain catalyst (Pd–Al_2O_3) and inert spheres. Due to the high activity of the catalyst, is more adequate for the RFR operation that this central section is formed by a mixture (50 vol.%) of catalyst and inert particles (refractory ceramic spheres of the same diameter). The inert parts of the bed are considered to be formed by spherically shaped refractory ceramic material (Table 3).

Table 2
Correlations used for the estimating kinetic and internal mass transfer parameters in the performed simulations

	Particle bed	Structured bed
Surface–volume ratio	$a_G = 6/d_P\ (1-\varepsilon)/\varepsilon$; $a_S = 6d_P$	$a_G = 4/D_H$; $a_S = 4/D_H(\varepsilon/1-\varepsilon)$
Kinetic constant per catalyst surface (k_S) and volume (k_{VC})	$k_S^{he} = (f_C/a_S)k_{VC}$	$k_S^{he} = L_C k_{VC}$
Reaction internal effectiveness	$\eta = 3/\phi\ ((1/\tan h\phi) - (1/\phi))$	$\eta = \tan h(\phi)/\phi$
Thiele modulus	$\phi = d_{PC}/2\sqrt{k_{VC}/D_{eff,pores}}$	$\phi = L_C\sqrt{k_{VC}/D_{eff,pores}}$

Table 3
Solid physical properties for particle and structured beds

	Particle bed		Structured bed catalyst and inert (cordierite)
	Catalyst ($Pd–Al_2O_3$)	Inert (refractory ceramic)	
Density, ρ (kg/m^3)	1257	2000	2500
Heat capacity, C_P (J/kg K)	836	890	965
Thermal conductivity, k (W/m K)	0.042	1.13	2.15
Bed porosity (ε)	0.36	0.36	0.66
Thermal capacity per reactor volume $(1-\varepsilon)\ \rho_S C_{PS}$ (MJ/m^3 reactor K)	0.67	1.14	0.82

The structured bed is considered to be formed by modular monoliths of cordierite, coated with $Pd–Al_2O_3$ only in the central section of the bed. Thus, in this case the physical properties remain constant along the reactor (Table 3).

Since the gas flowing through the monolithic bed is not in direct contact with the reactor wall, the gas-wall heat transfer coefficient in this case is equal to zero, and the heat transport from the monolith to the reactor wall takes place thought an insulation layer with thickness 5mm and thermal conductivity 0.042 W/m K.

The transport coefficients used to simulate the particle bed reactor were experimentally validated and reported in a previous work [9], whereas for the structured bed reactor equations recommended in the bibliography [8,10] were employed.

2.4. Mathematical model solving

The mathematical model presented is formed by four partial differential equations and additional algebraic equations, from which, physical, chemical and transport properties are calculated. The solution of this model is performed using the 'method of lines', in which the system of partial differential equations is replaced by a system of ordinary differential equation that can be solved using several algorithms. The reactor is divided into a grid of intervals (100–300, depending on the complexity of the simulation) and then the space derivatives are replaced by finite differences into each interval.

In our case, a MATLAB code has been developed to solve this model. The program solves the system of ordinary differential equation derived from the mathematical model for a particle or structured fixed bed reactor, taking into account that the reactor feed flow is periodically reversed. This is done using sequentially the mathematical solver for solving the ordinary differential equation system in each flow way, just by changing the spatial coordinates.

Due to the large size of the resulting system of differential equations, the *ode*23*s* MATLAB code was used for its solution. This solver is based on the numerical differentiation formulas (NDFs) and is recommended when the problem is stiff or the standard solver is very inefficient. Moreover, the developed program provides a graphical user interface for data entry and for analyzing the results (post-processing).

As mentioned previously, the mathematical model was experimentally validated for the reverse flow reactor consisting of a particle bed formed by spherical catalyst and inert particles. Good agreement between experimental and simulated data (temperature profiles and outlet concentrations for a wide range of operating conditions) was observed. The mathematical model for the reverse flow reactor containing a structured catalyst bed has not been experimentally validated yet.

3. Results and discussion

The simulations were performed in order to compare the two reverse flow reactor configurations, particle and structured bed, in a wide range of operating conditions. The main parameters used for this comparison are the reactor stability (considering the maximum switching time that avoids the reactor extinction for a given methane concentration), maximum temperature in the catalytic bed (related to catalyst deactivation) and pressure drop in the bed.

The same reactor length and diameter were considered for both configurations, in order to maintain a similar influence of the reactor wall effects. The variables that were not changed throughout the simulations are shown in Table 1.

Due to the large number of variables involved in the operation of reverse flow reactors, it is necessary to limit the number of variables studied. In our case, the variables selected are surface velocity, particle diameter (or cell density for monolith), and fraction of the bed occupied by catalyst. This selection has been made considering that they are the most important parameters for process design and that they are the parameters with greater effect on the reaction kinetics and transport phenomena taking place in the reactor. Surface velocity (u_0) depends only on the feed flow rate and the reactor diameter. The particle diameter (d_P), which is the same for both the catalyst and inert materials, is very important, because it affects both mass and heat transfer. For the structured bed, the equivalent variable

Table 4
Numerical code for case studies reported in this paper

Case study	1	2
Superficial velocity (u_0)	0.1 m/s	0.3 m/s
Particle diameter (d_P) (only particle bed)	3 mm	6 mm
Cells density (N_m) (only structured bed)	400 cpsi (62 cells/cm^2)	200 cpsi (31 cells/cm^2)
Hydraulic diameter (D_H) (only structured bed)	1.16 mm	1.65 mm
Catalytic bed fraction on the entire reactor (f_{BC})	50%	30%

Table 5
Summary of the simulation results (see code for case study in text)

Case	u_0 (m/s)	d_P (mm)	N_m (cpsi)	f_{BC} (%)	Particle bed			Structured bed		
					$t_{SW,}$ (s)	$_{cr}t_{SW,\ 25\%}$ (s)	$_{cr}\Delta P/L$ (Pa/m)	$t_{SW,}$ (s)	$_{cr}t_{SW,\ 25\%}$ (s)	$_{cr}\Delta P/L$ (Pa/m)
111	0.1	3	400	50	3630	2723	944	2225	1669	100
112	0.1	3	400	30	3130	2348	1086	1700	1275	110
121	0.1	6	200	50	3050	2288	294	2100	1575	50
122	0.1	6	200	30	2625	1969	330	1600	1200	55
211	0.3	3	400	50	1230	923	4678	800	600	394
212	0.3	3	400	30	1085	814	5430	600	450	428
221	0.3	6	200	50	995	746	1672	710	533	166
222	0.3	6	200	30	860	645	1884	560	420	246

is the cell density (N_m), whose election determines also the monolith hydraulic diameter (D_H), as shown in Table 4. The selected values of the particle diameter and the cell density are commonly found in commercial catalysts. Finally the catalytic bed fraction on the entire reactor (f_{BC}) is the fraction of the reactor length occupied by the catalytic bed, the inert material occupying the remaining reactor volume. For each selected variable, two values were considered, resulting therefore eight (2^3) case studies, summarized in Table 4.

The stability curves (conversion versus switching time), depicted in Fig. 1 and summarized in Table 5, were obtained by simulating the behavior of the reverse flow reactor for each case study at different switching times (t_{SW}). It can be observed that there is a critical switching time ($t_{SW,cr}$), characteristic from each case study, above which the reverse flow reactor is unstable, headed to extinction. This critical switching time can be used to compare the stability of different RFR configurations.

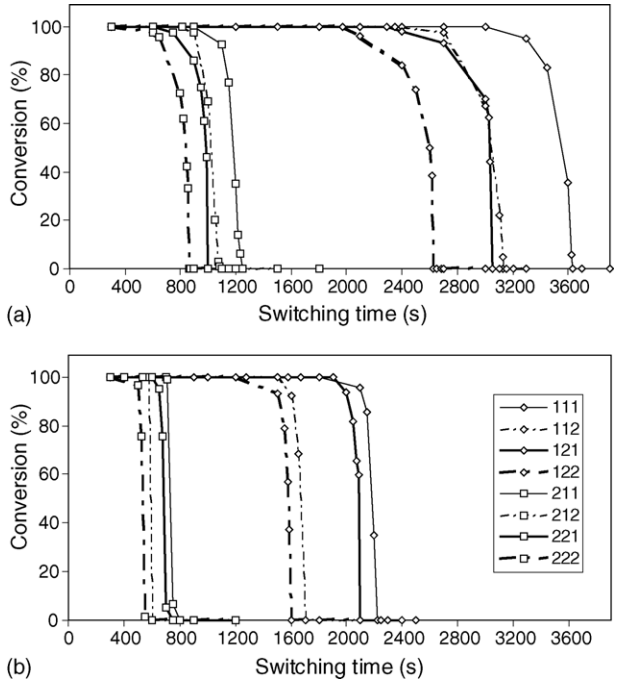

Fig. 1. Stability curves: (a) particle bed catalyst and (b) structured bed catalyst. Studied variables: surface velocity (◇: 0.1 m/s, ϒ: 0.3 m/s); particle diameter/cell density (thin line: 3 mm/400 cpsi, thick line: 6 mm/200 cpsi); catalytic bed fraction (—: 50%, – –: 30 %). See the codes of the legends at Table 5.

According to the results obtained several conclusions can be obtained: as general trend the stability of the monolithic bed is lower than the corresponding to the particle bed, although this difference tends to decrease as the gas surface velocity increases.

For both configurations, the reactor stability increases as surface velocity decreases. This effect can be explained by the increase of heat accumulation in the bed favoured by the lower convective heat transfer associated to low surface velocity. Concerning the particle size, small particle diameter leads to a more stable operation in the particle bed reactor, basically because of the resulting increase in mass transfer efficiency. Moreover, higher cell density in the structured bed (lower hydraulic diameter) leads also to a more stable operation. The effect of the inert fraction in the range considered is similar for both kinds of beds: the higher the inert fraction the higher the stability. The stability gain is more marked for the structured packing, which can be related to the lower thermal capacity per reactor volume of the structured bed in the inert sections. Then, an increase in the bed inert endings length has a stronger effect on the structured bed because the contribution to the thermal inertia is higher in relative terms.

Other aspect to be considered is the pressure drop in the bed. Pressure drops for the abovementioned simulations have been estimated using the Ergun and Hagen-Poiseuille equations for particle and structured bed, respectively [11]. Values of pressure drop given in Table 5, were calculated for a switching time 25% lower than the critical value. The values of the pressure drop are given per unit of reactor length, so as to facilitate the comparison, taking into account the length of reactor needed for getting a required performance. The pressure drops are significantly lower (one order of magnitude) in the case of the monolithic bed, being this difference higher as the surface velocity increases and as the particle diameter increases. As expected, an increase in cells density leads to a slight increase in pressure drop. Increasing the bed catalytic fraction leads to a decrease in the pressure drop through the bed. This effect could be caused by the lower average temperatures reached in the bed, since the reaction enthalpy is released on a larger amount of material.

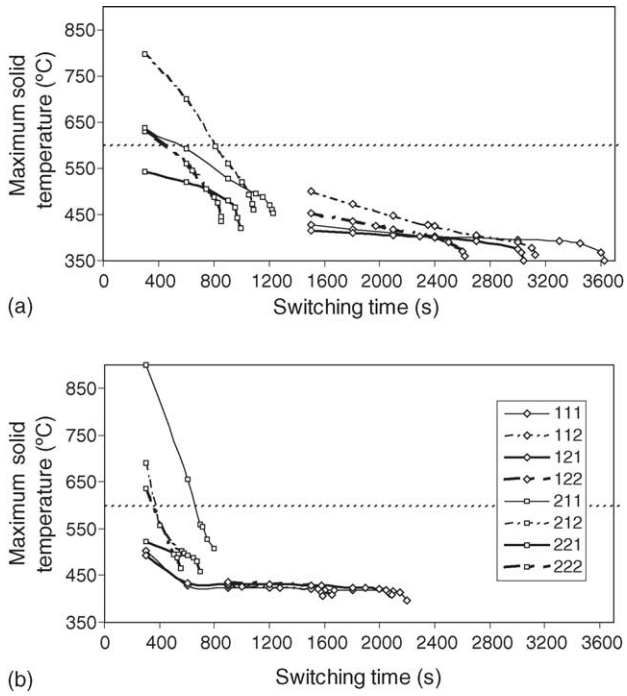

Fig. 2. Maximum solid temperature curves: (a) particle bed catalyst. (b) structured bed catalyst. Studied variables: surface velocity (◇: 0.1 m/s, ϒ: 0.3 m/s); particle diameter/cell density (thin line: 3 mm/400 cpsi, thick line: 6 mm/200 cpsi); catalytic bed fraction (—: 50%, – –: 30%). See the codes of the legends at Table 5.

Fig. 2 shows the maximum temperature attained by the catalyst at the pseudo-steady state versus the switching time. It can be observed that the solid temperature is higher in the case of high surface velocity, because the methane molar flow rate is also higher. As the catalyst deactivates at temperatures higher than 600 °C, the points above this value (corresponding to low switching times) must not be considered.

The simulations performed at the lowest surface velocity show a remarkable behaviour: before reaching the critical switching time, the temperature tends to a fixed value, which is not influenced by the catalytic bed fraction, the particle diameter or the cell density. This value is around 400 °C for the particle bed and 430 °C for the structured bed. If structured and particle beds are compared, the maximum temperatures are slightly higher in the structured bed.

In order to study the influence of each variable considered in Table 4 on the reactor stability, a multiple lineal regression analysis of the critical switching time has been done (Eq. (7)). The purpose of this analysis is to compare qualitatively the influence of the studied variables on the stability.

$$t_{SW,cr} = a_1 u_0 + a_2(d_P, N_m) + a_3 f_{BC} + a_0 \quad (7)$$

The calculated regression coefficients (a_i) reported in Table 6, are related to the individual contribution of each variable to the critical switching time. As the units of these coefficients are not uniform, and in order to facilitate the comparison, the coefficients have been transformed to uniform units ($\hat{a}_i$, seconds) by multiplying them by the lowest value of the corresponding variable. When the regression coefficient is negative, an increase in the corresponding variable will decrease the critical switching time, and hence the stability. According to the uniform coefficients, the variation of the creeping velocity of the heat wave caused by changes in the surface velocity prevails over the effects of the other two variables studied. This can also be observed in a qualitative way in Fig. 1, since the largest changes of stability take place for variations in the surface velocity.

Fig. 3 shows the methane concentration and solid temperature profiles along the reactor for both particle and structured catalyst beds, for the case study 121. Due to the different stability range of the two types of bed, previously discussed, the comparison is not possible for the same switching time, and a switching time 25% lower than the critical value for each bed type has been selected (2288 s for the particle bed and 1575 s for the structured bed). Methane concentration profiles (Fig. 3a and b) show that methane concentration decrease is more pronounced in the structured bed, because the reaction takes place in a smaller volume. As a result the reaction heat is also released in a smaller volume, producing a sharper solid temperature profile and higher maximum temperature for the structured bed (Fig. 3c and d). The thermal capacity per reactor volume $[(1-\varepsilon)\,\rho_S C_{PS}]$ relates the heat released with the temperature increment. The values of this property are shown in Table 3, being remarkable that the value for the structured bed is higher than for the catalyst packed bed, but lower than for the inert packed bed. This is explained considering the higher solid density of the structured packing, which overcompensates its higher void fraction. The sharper solid temperature profile and higher maximum temperature in the structured bed are produced by the higher reaction rate per unit volume (due to better intra-particle mass transfer).

Table 6
Regression parameters for the determination of the influence of the studied variables

	i	0	1	2	3	r^2	$(E_{Relatve})_{max}$ [a]
Particle bed	a_i	4119	−10330	−129	15	0.988	18.8%
	$\hat{a}_i$ (s)	4119	−1033	−386	452		
Structured bed	a_i	1705	−6194	0.44	17	0.983	19.4%
	$\hat{a}_i$ (s)	1705	−619	89	516		

See text for the units of unnormalized parameter.

[a] $(E_{relative})_{max} = |(t_{SW,cr})_{eq.(7)} - (t_{SW,cr})_{exp}/(t_{SW,cr})_{exp}|_{max} \times 100$.

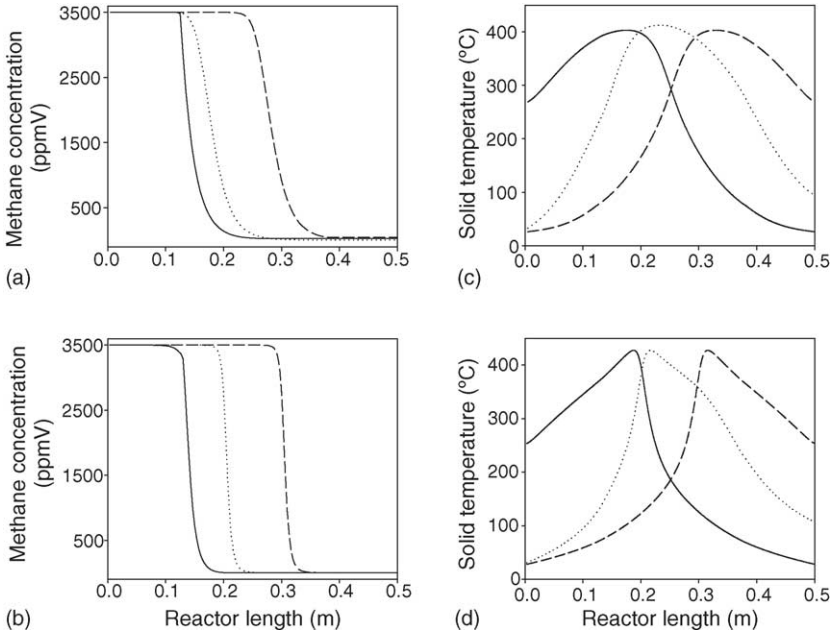

Fig. 3. Case study 121. Methane concentration profiles along the reactor: (a) particle bed; (b) structured bed. Solid temperature profiles along the reactor: (c) particle bed; (d) structured bed. Beginning (solid line), middle (dotted line) and end (dashed line) of a direct semicycle at the pseudo steady state.

4. Conclusions

The comparison of the performance of catalytic reverse flow reactors containing the catalyst, either as a packed bed or as monolith, shows that the particle bed performs better in terms of reactor stability. The difference between both configurations decreases as the surface velocity increases. Concerning to the maximum temperature reached in the catalytic bed, the behaviour of both types of beds is very similar, whereas the pressure drop is largely higher in the particle bed reactor. In spite of its lower stability range, results indicate that monolithic reverse flow reactors can perform adequately, and are a very interesting alternative for large-scale reactors. This is mainly due to the lower pressure drop, but there are also other favorable characteristics, such as the higher intraparticle effectiveness factor, and higher solid density.

Acknowledgements

This work was financed by a Research Project of the Regional Plan for Research, Development and Innovation of the Regional Asturian Government (Spain) (FC-03-PB02-133).

References

[1] P. Artizzu, E. Garbowski, M. Primet, Y. Brulle, J. Saint-Just, Catal. Today 47 (1999) 83–93.
[2] D. Fissore, A.A. Barresi, Chem. Eng. Res. Des. Trans. IChemE Part A 81 (2003) 611–617.
[3] Y.S. Matros, G.A. Bunimovich, Catal. Rev. Sci. Eng. 38 (1996) 1–68.
[4] G. Eigenberger, U. Nieken, Int. Chem. Eng. 34 (1994) 4–16.
[5] M.A.G. Hevia, D. Fissore, S. Ordóñez, F.V. Díez, A.A. Barresi, CHISA 1.158, Prague, (2002).
[6] B. Lui, R.E. Hayes, M.D. Checkel, M. Zheng, E. Mirosh, Chem. Eng. Sci. 56 (2001) 2641–2658.
[7] R.E. Hayes, S.T. Kolaczkowski, P.K.C. Li, S. Awdry, Applied Catal. B 25 (2000) 93–104.
[8] R.E. Hayes, S.T. Kolaczkowski, Introduction to Catalytic Combustion, first ed., Gordon and Breach Science Publishers, 1997 (Chapter 3), p. 314 and 333.
[9] D. Fissore, A.A. Barresi, G. Baldi, M.A.G. Hevia, S. Ordoñez, F.V. Díez, AIChE J. 51 (6) (2005) 1654.
[10] R.D. Hawthorn, AICheE. Symp. Ser. 70 (137) (1974) 428.
[11] R.B. Bird, W.E. Stewart, E.N. Ligthfoot, Transport Phenomena, John Wiley and Sons, 1960, p. 188 and 200.